Wave properties in the magnetic reconnection diffusion region with high β: Application of the k-filtering method to Cluster multispacecraft data

S. Y. Huang,[1] M. Zhou,[1,2] F. Sahraoui,[3,4] X. H. Deng,[1,2] Y. Pang,[1,2] Z. G. Yuan,[1] Q. Wei,[1] J. F. Wang,[1] and X. M. Zhou[1]

Received 4 February 2010; revised 24 July 2010; accepted 3 September 2010; published 4 December 2010.

[1] Magnetic reconnection is a crucial physical process in laboratory and astrophysical plasmas. Plasma waves are believed to provide the dissipation mechanism in magnetic reconnection. In this paper we analyze the properties of low-frequency waves in a magnetotail reconnection diffusion region with a small guide field and high β. Using the k-filtering method on the magnetic field data measured by Cluster spacecraft, we found that low-frequency waves in the diffusion region were highly oblique propagating mode. We compared the measured dispersion relation with theoretical ones calculated using the linear (hot) two-fluid and Vlasov-Maxwell theory. It is found that the observed waves in the diffusion region (with high plasma β) follow the dispersion relation of the Alfvén-Whistler wave mode. Comparisons with previous simulations and observational results are also discussed.

Citation: Huang, S. Y., M. Zhou, F. Sahraoui, X. H. Deng, Y. Pang, Z. G. Yuan, Q. Wei, J. F. Wang, and X. M. Zhou (2010), Wave properties in the magnetic reconnection diffusion region with high β: Application of the k-filtering method to Cluster multispacecraft data, *J. Geophys. Res.*, *115*, A12211, doi:10.1029/2010JA015335.

1. Introduction

[2] Magnetic reconnection is a very important physical process in astrophysical and laboratory plasmas, which enables reconfiguration of the magnetic field topology and converts the magnetic field energy to plasma kinetic and thermal energy. The diffusion region is a crucial region of reconnection where magnetic field and plasma decouple from each other and strong wave activity and complex wave-particle interactions occur [e.g., *Deng and Matsumoto*, 2001; *Vaivads et al.*, 2006].

[3] MHD models of reconnection require sufficient resistivity to achieve fast reconnection. However, collisional resistivity in collisionless plasma is negligible, thus it has been suggested that fast reconnection can be achieved by anomalous resistivity due to wave-particle interactions in the diffusion region. This may involve, for instance, lower hybrid waves, which have been suggested to play that role in the reconnection region [*Labelle and Treumann*, 1988; *Cattell et al.*, 1995; *Vaivads et al.*, 2006]. However, in situ measured anomalous resistivity arising from lower hybrid waves in the diffusion region cannot balance the reconnection inductive electric field [*Bale et al.*, 2002; *Eastwood et al.*, 2009; *Zhou et al.*, 2009].

[4] In contrast, it is well known that the diffusion region exhibits two characteristic scales, the ion diffusion region and the electron diffusion region, owing to the decoupling of ion and electron motion [*Sonnerup*, 1979]. The decoupling of ions and electrons in the diffusion region results in Hall currents. Recent numerical simulations have shown that Hall effects allow the reconnection rate to be controlled solely by the ion dynamics, and the mechanism required to break the frozen-in condition in the electron diffusion region plays no role [*Birn et al.*, 2001]. The predicted reconnection rate based on models that include the Hall effect has been estimated as ~0.03–0.2 v_{in}/v_{uA} (v_{in} and v_{uA} being, respectively, the inflow speed and the upstream Alfvén speed) [*Wang et al.*, 2006], which has been confirmed by recent satellite observations [*Vaivads et al.*, 2004; *Xiao et al.*, 2007]. Moreover, electron dynamics in the ion diffusion region are governed by whistler waves and/or kinetic Alfvén waves (KAWs), implying that fast reconnection is mediated by dispersive waves [*Rogers et al.*, 2001]. Whistler waves were first reported in the vicinity of reconnection diffusion region in the Earth's magnetosphere by *Deng and Matsumoto* [2001]. *Eastwood et al.* [2009] also reported wave activity within a reconnection diffusion region without a guide field and found it to be consistent with parallel-propagating whistler waves. KAWs were suggested to play important roles in fast magnetic reconnection in the magnetosphere [*Chaston et al.*, 2005,

[1]School of Electronics Information, Wuhan University, Wuhan, China.
[2]Also at Institute of Space Science and Technology, Nanchang University, Nanching, China.
[3]NASA Goddard Space Flight Center, Greenbelt, Maryland, USA.
[4]Also at Laboratoire de Physique des Plasmas, CNRS-Ecole Polytechnique, Observatoire de Saint-Maur, Saint-Maur, France.

Copyright 2010 by the American Geophysical Union.
0148-0227/10/2010JA015335

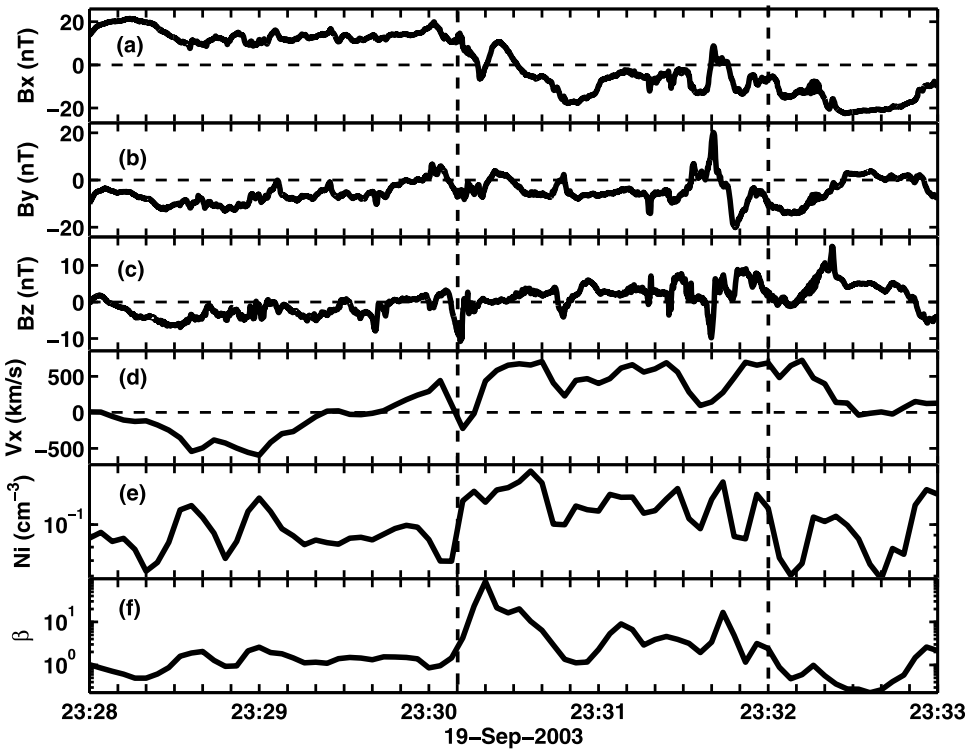

Figure 1. Overview of Cluster 4 observations in the diffusion region encountered between 2328 and 2333 UT: (a–c) three components of the magnetic field, (d) X component of the proton bulk velocity, (e) proton density, and (f) plasma β. The two vertical dashed lines show the time interval during which the k-filtering technique was applied.

2009] and in energy dissipation at the electron scale in solar wind turbulence [*Sahraoui et al.*, 2009].

[5] Since most of the magnetic field energy is stored in the low-frequency part of the fluctuations, it is necessary to investigate the nature of low-frequency waves in the diffusion region to fully understand their role in the mechanisms of reconnection. Here we present a study of wave properties in a high-β-diffusion region with a small guide field based on Cluster observations on 19 September 2003. *Borg et al.* [2005] and *Chaston et al.* [2009] have studied this event and confirmed that the Cluster spacecraft encountered a diffusion region around 2330 UT. *Chaston et al.* [2009] have, furthermore, estimated the wave vectors of the fluctuations using an interferometry method that makes use of measured phase differences between the satellites [*Walker et al.*, 2004]. They showed that waves observed in the diffusion region were consistent with KAWs. We use a more robust method, namely, the k-filtering technique, to study the properties of low-frequency waves observed by the Cluster spacecraft and compare them to the results of *Chaston et al.* [2009]. The k-filtering technique is a generalized minimum variance technique introduced into space science by *Pinçon and Lefeuvre* [1991]. This technique allows one to estimate the magnetic wave field energy distribution $\mathbf{P}(\omega, \mathbf{k})$ in the frequency and wave vector domain from data measured simultaneously at several points in space, under the assumption of (sufficient) stationarity of the time series (more details on this technique are given by *Pinçon and Lefeuvre* [1991], *Pinçon and Motschmann* [1998], *Sahraoui et al.* [2003, 2010], *Tjulin et al.* [2005], and *Narita et al.* [2010]). High-resolution data from the Cluster spacecraft is used for this analysis. The FluxGate Magnetometer (FGM) instrument provides 22 Hz magnetic field data [*Balogh et al.*, 1997], and the Electric Fields and Waves (EFW) instrument provides 25 Hz electric field data [*Gustafson et al.*, 1997]. Plasma data on ions and electrons (with 4 s resolution) were obtained from the Cluster Ion Spectrometry (CIS) and plasma electron and current experiment (PEACE) instruments, respectively [*Rème et al.*, 2001; *Johnstone et al.*, 1997].

2. Overview of the Cluster Observations

[6] Figure 1 shows the observations of Cluster C4 during the crossing of a reconnection diffusion region on 19 September 2003 from 2328 to 2333 UT, when Cluster was located near (−17.4, 3.7, 0.5) R_E (Earth radius) in the geocentric solar magnetospheric (GSM) coordinates. It is worth noting that during this interval the current sheet coordinate is fairly close to the GSM coordinates [*Borg et al.*, 2005]. Therefore, we present all data in the GSM coordinates, unless otherwise specified. Large bulk flows were observed during this time interval (Figure 1d), with a maximum exceeding 500 km/s. The bulk flow reversal from tailward to earthward was detected from 2329:00 to 2330:15 UT, and the magnetic field B_z component (Figure 1c) reversed from negative to positive coincidently, which implies that the spacecraft moved from the tailward ($v_x < 0$) to the earthward ($v_x > 0$) side of an X line. *Borg et al.* [2005] have analyzed the magnetic and electric field perturbations and found them to be consistent with Hall effects predicted by numerical

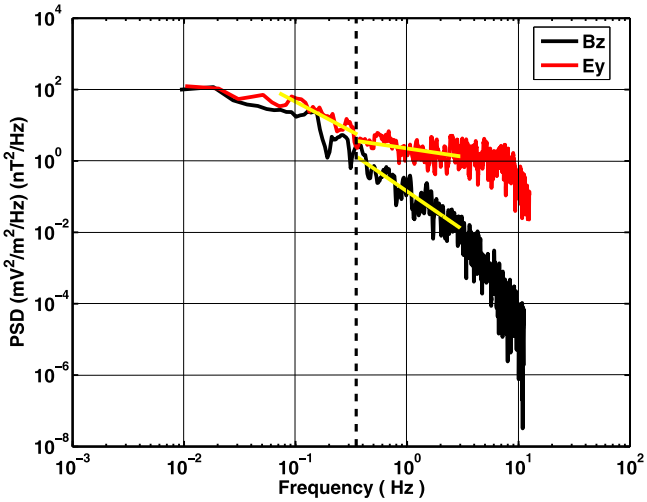

Figure 2. A log-log power spectral density (PSD) of E_y and B_z of Cluster 4 measured between 2330:10 and 2332:00 UT. E_y and B_z are shown in the DSI and the GSE coordinates, respectively. The vertical dashed line indicates the frequency at which the PSDs of E_y and B_z diverge. Yellow lines are direct power-law fits.

simulations [*Pritchett*, 2001; *Sonnerup*, 1979]. All the foregoing evidence indicates that the Cluster was located in the diffusion region. The detailed structure of this diffusion region was reported by *Borg et al.* [2005] and *Chaston et al.* [2009]. The plasma parameter β was much greater than 1 between 2330:15 and 2331:40 UT, meaning that the spacecraft was in the central current sheet (Figure 1f). During the earthward flow the proton density increased to 0.2 cm^{-3} (Figure 1e) and the plasma β was greater than 1; the magnetic and electric fields showed large fluctuations as well. The strength of the guide field throughout the diffusion region was about 1 nT, which represents 4% of the asymptotic magnetic field [*Borg et al.*, 2005]. During the earthward flow the averaged B_y gives a guide field strength of about −3.2 nT, which is 13% of the asymptotic magnetic field. In this paper we analyze the waves observed between 2330:10 and 2332:00 UT, when the Cluster was located on the earthward side of the X line.

[7] Figure 2 shows the power spectral density (PSD) of the magnetic and electric field measured by Cluster C4 between 2330:10 and 2332:00 UT. The electric field is presented in the spin plane (DSI), while the magnetic field is presented in the GSE coordinates. The PSDs were calculated using the multitaper method [*Percival and Walden*, 1993] as by *Eastwood et al.* [2009]. At a low frequency ($f_{sc} < 0.35$ Hz), the two PSDs show a similar trend (or scaling). Above 0.35 Hz (which is higher than the local ion cyclotron frequency of 0.1 Hz), the two PSDs diverge: the PSD of the electric field shows an enhancement between 1.5 and 6.5 Hz, while the PSD of the magnetic field decays. The frequency of the enhanced electric field approaches the lower hybrid frequency and is probably due to the lower hybrid drift waves [*Zhou et al.*, 2009]. The power law fit shows that the power law index between 0.07 and 0.35 Hz is about −5/3, which suggests viewing these frequencies (and the corresponding scales) as obeying the classical scenario of Kolmogorov turbulence [*Kolmogorov*, 1941]. The electric field follows a −1/2 power law, and the magnetic field follows a −2.15 power law between 0.35 and 3 Hz. Similar observations have been reported in the solar wind and in the magnetotail [*Bale et al.*, 2005; *Chaston et al.*, 2009; *Sahraoui et al.*, 2009].

3. Wave Analysis Using the *k*-Filtering Technique

[8] To estimate the experimental dispersion relations of the waves, we apply the k-filtering technique to the interval of earthward flow shown in Figure 1 and follow the approach introduced by *Sahraoui et al.* [2003]. To ensure the good quality of the estimation of the k vectors, the Cluster spacecraft must form a regular three-dimensional (3-D) tetrahedron in space [*Sahraoui et al.*, 2003, 2010]. This geometry is shown to be controlled by two parameters, namely, elongation E and planarity P [*Robert et al.*, 1998]. $P \sim 1$ reflects a "pancake" shape of the spacecraft, whereas $E = 1$ reflects a "cigar" configuration; values of these factors close to 0 are the ideal 3-D configuration required to use the k-filtering properly. In the present event we have $P \approx 0.27$ and $E \approx 0.21$, which ensures relatively good 3-D space coverage of the waves.

[9] The k-filtering method assumes that all the waves existing in the analyzed data have wavelengths larger than the average spacecraft separations. This allows one to define the wave number space accessible to measurements given by $k_{max} = 2\pi/\lambda_{min} \approx \pi/d$, where d is the average separation between the satellites in a given direction. Consequently, all the accessible wave numbers are assumed to belong to $[-k_{max}, k_{max}]$.

[10] We emphasize that limiting the interval of analysis to $[-k_{max}, k_{max}]$ does not allow one to avoid the spatial aliasing effect [*Sahraoui et al.*, 2003]. To minimize, or ideally suppress, this effect, one must limit the interval of frequencies to analyze to a range defined by the shortest wavelength given here and an existing characteristic velocity of the medium. If V_ϕ and V_f are the phase speed of waves and the flow speed, respectively, then the maximum frequency (in the satellite frame) accessible to analysis can be estimated from $f_{max} \approx k_{max}(V_\phi + V_f)/2\pi$ [*Sahraoui et al.*, 2003, 2010].

[11] During the experimental measurements used in this study, the Cluster satellites were separated by average distances of 146, 120, and 183 km in the x, y, and z directions of the GSM coordinate, which yield average maximum wave vector components $k_{max} \approx (0.0214, 0.0261, 0.0171)$ rd/km. In the time interval of interest the average magnetic field was [−4.7, −4.1, 2.2] nT, the plasma density was about 0.13 cm^{-3}, the average plasma flow vector was [445, −71, 303] km/s, the proton temperature was $T_i \sim 7570$ eV, and the electron temperature was $T_e \sim 2500$ eV. This yields an ion gyrofrequency $f_{ci} \sim 0.1$ Hz, an ion thermal speed $V_{th} \sim 1210$ km/s, an Alfvén speed $V_A \sim 655$ km/s, and a plasma $\beta \sim 3.4$. If we assume that the waves have a phase speed $V_\phi \sim V_A$, then the maximum frequency (in the spacecraft reference frame) accessible to the k-filtering analysis is $f_{max} \sim k_{max}V_A/2\pi \sim 2$ Hz.

[12] Figure 3 shows a 2-D view of the magnetic wave field energy distribution for different frequencies in the spacecraft frame in the plane (k_x, k_y) for a given k_z plane corresponding to the maximum energy for each frequency.

The frequency $f = 0.35$ Hz is the one for which the PSDs of E_y and B_z diverge. In each graph we overplot the Doppler shift curve $\omega = \mathbf{k} \cdot \mathbf{V}_f$ (blue line) and the Doppler-shifted dispersion relations of the low-frequency plasma modes calculated using the Hall-MHD approximation (red curves). These dispersion relations were calculated using the measured plasma parameters already given. Because the frequencies are measured in the spacecraft frame, while the

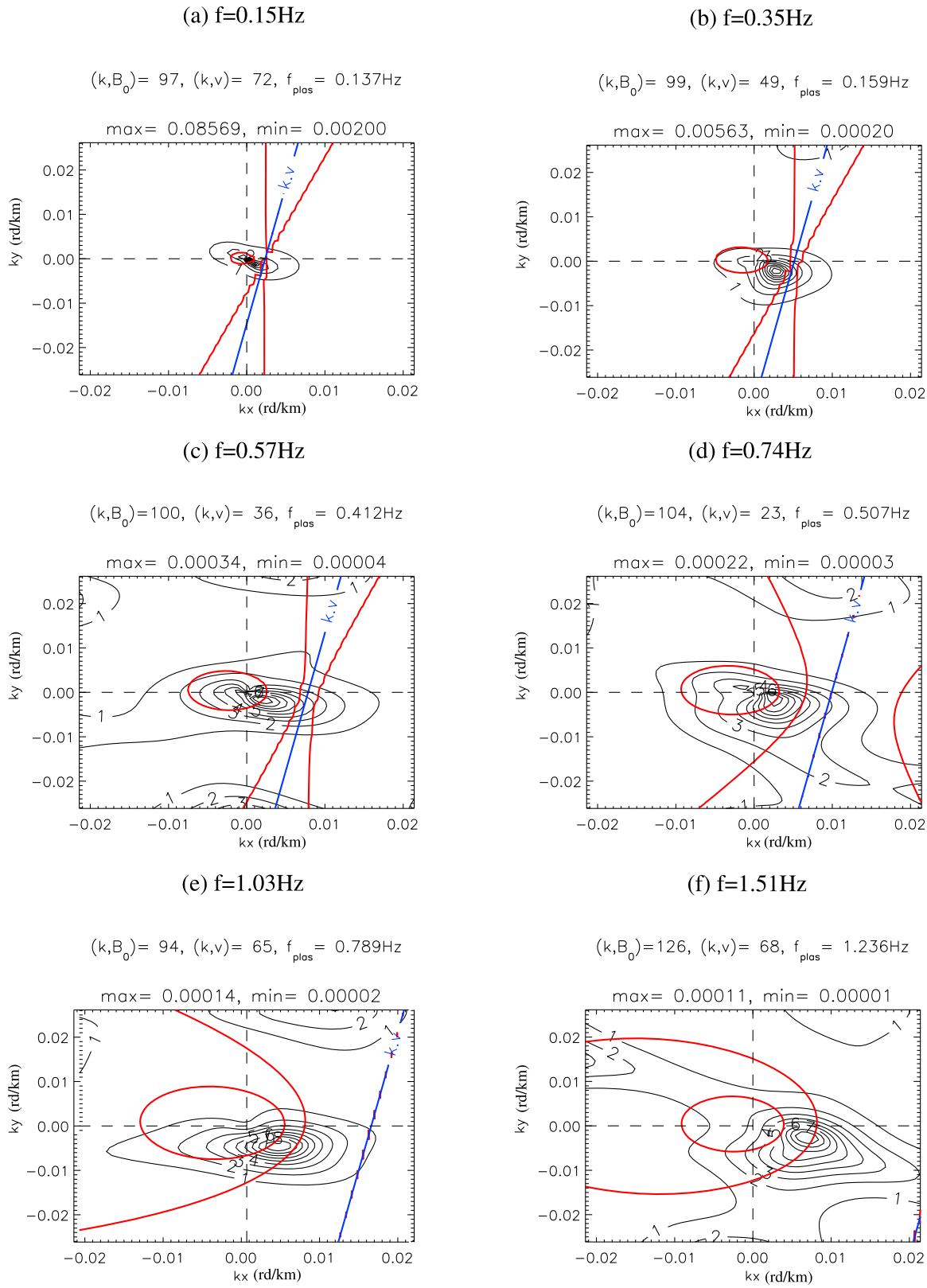

Figure 3

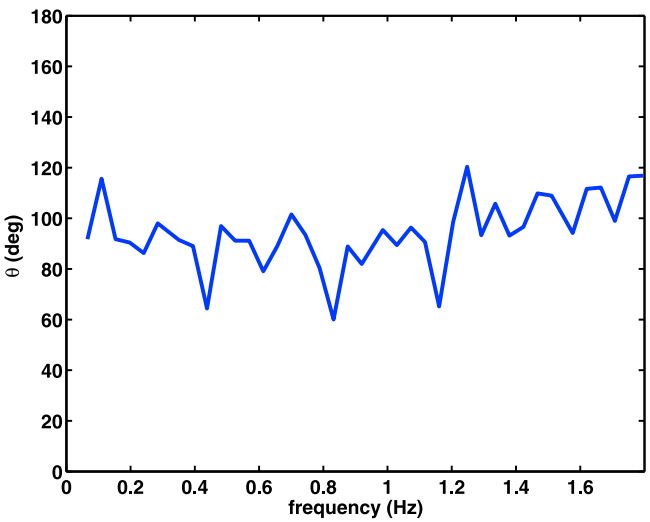

Figure 4. The angles between the identified wave vectors and the ambient magnetic field for each studied frequency in the spacecraft frame.

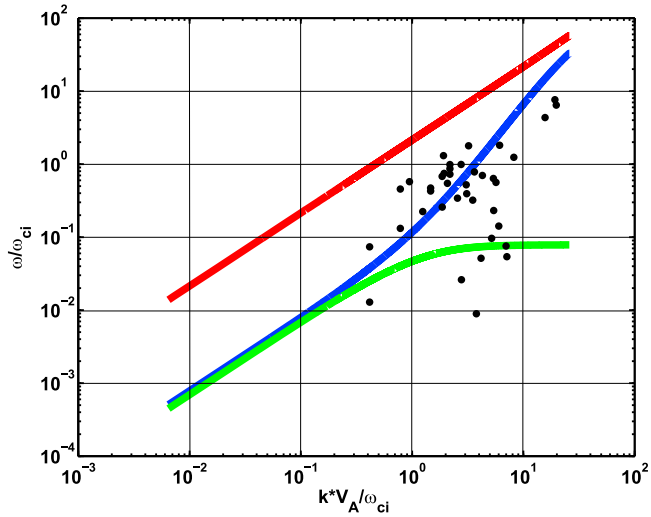

Figure 5. Comparison between the measured dispersion relation (filled circles) and the theoretical ones deduced from the hot two-fluid equations in the plasma frame. Red, blue, and green lines are the fast, intermediate, and slow modes, respectively. Frequencies are normalized by the ion cyclotron frequency ω_{ci}, while wave vectors are normalized by ω_{ci}/v_A, where $v_A \approx 655$ km/s is the local Alfvén speed.

theoretical dispersion relations are in the plasma rest frame, one needs to transform them to the same reference frame. Here we choose to Doppler-shift the theoretical dispersion relations using the equation $\omega_{plas} = \omega_{sc} - \mathbf{k} \cdot \mathbf{V}_f$, where $\mathbf{k}$ is the wave vector estimated by the k-filtering, ω_{sc} and ω_{plas} are the frequencies in the spacecraft and the plasma rest frames, respectively, and $\mathbf{V}_f$ is the plasma bulk velocity. The results are shown for six frequencies belonging to the interval just defined: $f = 0.15$ Hz (Figure 3a), $f = 0.35$ Hz (Figure 3b), $f = 0.57$ Hz (Figure 3c), $f = 0.74$ Hz (Figure 3d), $f = 1.03$ Hz (Figure 3e), and $f = 1.51$ Hz (Figure 3f). In Figure 3a the energy peak is found near the $\mathbf{k}$ vector forming an angle $\theta \approx 97°$ with the ambient magnetic field. The peak lies between the dispersion relation of the fast mode and that of the Alfvén modes. Results for higher frequencies shown in Figure 5 provide evidence of a statistical agreement with the dispersion relation of the Alfvén mode computed from the fluid theory. This will be confirmed by comparison to the exact dispersion relations and damping rate from the linear Vlasov-Maxwell equations.

[13] Figure 4 shows the angles between the identified wave vectors with respect to the ambient magnetic field for a series of frequencies. We found that the wave vectors for frequencies below 1.8 Hz primarily propagate between 60° and 120° with respect to the ambient magnetic field B_0, with an average value of about 95°, implying that the waves are highly oblique propagating modes. Note that for all frequencies studied here (up to 1.8 Hz) the energy peaks considered have intensities at least four times higher than background energy (in other words, maximum/minimum energy ratios >4). We also found that the wave vectors have a large $+k_y$ component, but the waves were propagating in the positive X direction (GSM), away from the X line.

[14] Figure 5 shows the measured dispersion relations using the k-filtering technique and the theoretical ones derived from the hot two-fluid approximation in the high-β case [*Formisano and Kennel*, 1969]. We used $\beta \sim 3.4$ and a propagation angle of 95° to calculate the theoretical dispersion solutions. We can see that the measured dispersion relation generally follows the "intermediate" mode (defined as the extension of the Alfvén mode to higher frequencies). We note, however, a slight spread of the experimental dispersion relation at very low frequencies.

[15] The wave modes calculated from the two-fluid approximation (Figure 5) may be affected by the cyclotron and/or Landau damping. To take into account this possible damping, one needs to compare observations with the kinetic theory. For this purpose we solve the linear Maxwell-Vlasov equations using the WHAMP (waves in homogeneous anisotropic multi-component plasmas) code [*Rönnmark*, 1982] under the same plasma parameters and propagation angle already given. We assume that the ions and electrons

Figure 3. Black curves are two-dimensional views of the magnetic field energy distribution for a k_z plane corresponding to the maximum energy calculated by the k-filtering method. Six frequencies (in the spacecraft reference frame) are represented: (a) $f = 0.15$ Hz, (b) $f = 0.35$ Hz, (c) $f = 0.57$ Hz, (d) $f = 0.74$ Hz, (e) $f = 1.03$ Hz, and (f) $f = 1.51$ Hz. Red curves are the Doppler-shifted theoretical dispersion relations from the Hall-MHD approximation. The blue line is the Doppler shift $\omega = \mathbf{k} \cdot \mathbf{V}_f$ (corresponding to stationary structures in the plasma rest frame, $\mathbf{k}$ is the wave vector estimated by the k-filtering method in the GSM coordinate, and $\mathbf{V}_f$ is the plasma bulk velocity measured by the CIS instrument). "max" and "min" indicate the maximum and the minimum energy density for the given k_z plane (nT^2/Hz (rd/km)^3). ($\mathbf{k}$, B_0) and ($\mathbf{k}$, $\mathbf{V}_f$) are the angles formed by the $\mathbf{k}$ vector with the ambient magnetic field B_0 and with $\mathbf{V}_f$. f_{plas} is the Doppler-shifted frequency in the plasma frame.

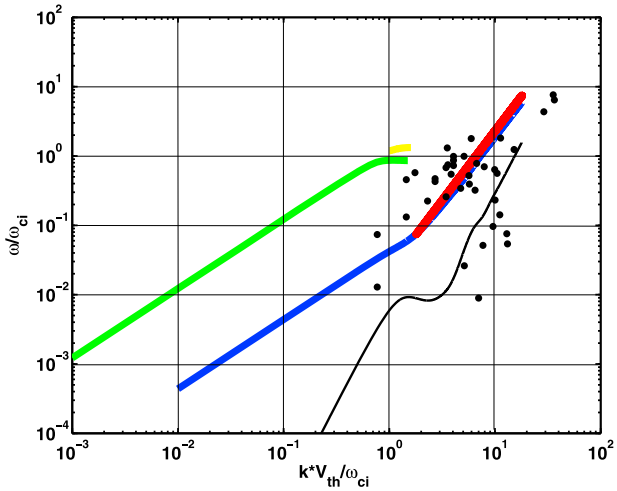

Figure 6. Comparison between the linear solutions of the Vlasov-Maxwell equations (colored curves) and the measured dispersion relation in the plasma frame (filled circles). Yellow, green, and blue curves are the Bernstein, fast, and Alfvén modes, respectively. The red curve represents the equation $\omega/k^2 \approx |\cos\theta| v_A^2/\omega_{ci}$. The black curve is the damping rate of the Alfvén-whistler mode, normalized by the ion cyclotron frequency ω_{ci} (i.e., $|\gamma|/\omega_{ci}$).

have isotropic Maxwellian distributions. Figure 6 displays the solutions obtained compared to the k-filtering results. Again, we found that almost all points follow the intermediate mode at higher frequencies, which is consistent with previous results from the fluid theory. The intermediate mode is only slightly damped at higher frequencies since the average ratio $|\gamma|/\omega_r$ is about 0.1, with a maximum of less than 0.25 (γ is the damping rate and ω_r is the real part of the frequency), which suggests that this wave mode is likely to be observed in the diffusion region. We note that, under the present condition of a high β and high oblique propagations, the fast magnetosonic mode splits into Bernstein modes [*Grison et al.*, 2005; *Howes*, 2009].

4. Discussion and Conclusion

[16] The classical MHD-like modes, that is, the fast, Alfvén, and slow modes, have very different physical properties, depending on the value of the plasma β. In the high-β case the two-fluid dispersion relation has two solutions at high frequencies ($\omega/\omega_{ci} > 1$). One is the electroacoustic mode, which extends the fast mode at high frequencies (red curve in Figure 5). This mode satisfies $\omega/k \approx C_s$, where C_s is the sound speed. In the limit $T_e \ll T_i$ (or in the monofluid description such as the Hall-MHD), this dispersion relation tends to $\omega/k \approx V_{thi}$, where V_{thi} is the ion thermal speed. In the quasi-parallel propagation ($k \sim k_{||}$), this mode is strongly damped by the Landau effect and, consequently, becomes unlikely to be observed in high-β plasma. In a highly oblique propagation (i.e., $k_\perp \gg k_{||}$), the fast mode splits around the proton gyroharmonics into Bernstein modes [*Howes*, 2009], and therefore it cannot account for magnetic fluctuations above the proton gyrofrequency as we observed here. The second solution of the two-fluid equations is the intermediate mode, which is connected to the slow mode below the ion cyclotron frequency. It is worth noting that in the limit $\beta \gg 1$, the slow mode becomes rather Alfvénic and obeys the dispersion relation $\omega/k \approx |\cos\theta| v_A$. Therefore, the two modes (slow and shear Alfvén) become nearly degenerate at low frequencies as shown in Figure 5 [*Sahraoui et al.*, 2007]. A fit of the dispersion relation of the intermediate mode for $\omega/\omega_{ci} > 0.1$ (not shown here) yields is $\omega/k^2 \approx |\cos\theta| v_A^2/\omega_{ci}$, where θ is the wave normal angle relative to the ambient magnetic field, which is the classical asymptotic whistler branch. Hence, the name "Alfvén-whistler" was given to this mode [*Wang et al.*, 2000]. The exact dispersion relations computed form kinetic theory corroborated these results.

[17] Our results are supplements to the results obtained by *Eastwood et al.* [2009], who have shown that, in the reconnection diffusion region, low-frequency fluctuations for parallel propagation are carried by whistler modes. The difference between these two cases may arise from the difference in the plasma β and guide field strength in these two events. According to *Rogers et al.* [2001], the presence of dispersive wave with $v \propto k$ in the diffusion region depends on the three scales, d_s, d_e, and d_k, which yields to two independent parameters, $\mu_k = d_e^2/d_k^2$ and $\beta_k/2 = d_s^2/d_k^2$, and four regimes (see Figure 2 of *Rogers et al.* [2001]). In the event studied by *Eastwood et al.* the two parameters are approximately $\mu_k \sim 0 \ll 1$ and $\beta_k/2 \sim 0.5 < 1$, which favors the whistler mode. In our event we have $\mu_k \sim 0.028 \ll 1$ and $\beta_k/2 \sim 41 \gg 1$, for which both high- and low-frequency branches, that is, whistler wave and KAW modes, are allowed.

[18] As mentioned previously, *Chaston et al.* [2009] have investigated the same event and identified the waves in the diffusion region as KAWs. They showed that the KAWs propagate with phase fronts expanding from the X line in both the X and the Z directions, with k vectors having large out-of-plane components. These results are consistent with our observations. However, *Chaston et al.* found that the KAWs have frequencies such that $\omega/\omega_{ci} < 1$, which is not in agreement with our measurements: we found that KAWs extend above $\omega/\omega_{ci} \sim 1$ and may reach $\omega/\omega_{ci} \sim 8$. These discrepancies may have different origins. First, there is a difference between the time interval of *Chaston et al.* [2009] (2328:30–23:3230 UT) and ours (2330:10–2332:00 UT). The whole interval used by *Chaston et al.* [2009] involved flow reversal, which makes any estimation of the average flow speed (to correct from the Doppler shift) highly uncertain. Our time interval is shorter and is free of such reversals, which yields a more accurate estimation of the average flow speed. Second, there are intrinsic differences between the two methods (the k-filtering and the phase difference) used to estimate the characteristic of the waves [*Walker et al.*, 2004]. For instance, *Chaston et al.* [2005] claim to resolve scales smaller than the spacecraft separations and also analyzed frequencies up to 10 Hz in the spacecraft frame (these limits were not discussed by *Chaston et al.* [2009]), which most likely involve spatial aliases as shown by *Sahraoui et al.* [2010]. In our analysis the shortest wavelength analyzed was twice the spacecraft separation, and the highest frequency analyzed was $f_{max} \sim 2$ Hz. We note also that *Chaston et al.* estimated the frequencies of the waves (in the plasma rest frame) using an approximated dispersion relation, while we estimated the frequencies ω_{plas} directly from $\omega_{plas} = \omega_{sc} - \mathbf{k} \cdot \mathbf{V}_f$. These discrepancies will be investigated further in a future work.

[19] In summary, we study wave properties in a reconnection diffusion region encountered by the Cluster spacecraft. The reconnection diffusion region is characterized by a small guide field and a high plasma β. Using the k-filtering technique, we measured the wave vectors in the low-frequency range and found that the waves were highly oblique propagating modes. The measured dispersion relation was found to lie close to the Alfvén-whistler wave branch calculated using the hot two-fluid approximation and the kinetic theory. The relatively slight damping of this mode, estimated from the kinetic theory, supports our interpretation of the observed waves as Alfvén-whistler modes. Which waves dominate the reconnection layer with a strong guide field and low β and what role they might play in reconnection are further questions that will be investigated via satellite observations and kinetic simulations.

[20] **Acknowledgments.** We thank the Cluster teams (FGM, CIS, EFW, and PEACE) and Cluster Active Archive for the high-quality data and successful operation. This work is supported by the National natural Science Foundation of China (NSFC) under grants 40890163, 40574073, 40574074, 40640420563, 40325012, and by the key project of Ministry of Education of China under grant 307019. Philippa Browning thanks the reviewers for their assistance in evaluating the manuscript.

References

Bale, S. D., F. S. Mozer, and T. Phan (2002), Observation of lower hybrid drift instability in the diffusion region at a reconnecting magnetopause, *Geophys. Res. Lett.*, *29*(24), 2180, doi:10.1029/2002GL016113.

Bale, S. D., P. J. Kellogg, F. S. Mozer, T. S. Horbury, and H. Rème (2005), Measurement of the electric fluctuation spectrum of magnetohydrodynamic turbulence, *Phys. Rev. Lett.*, *94*, 215002–215002.

Balogh, A., et al. (1997), The Cluster Magnetic Field Investigation, *Space Sci. Rev.*, *79*, 65–91.

Birn, J., et al. (2001), Geospace environment modeling (GEM) magnetic reconnection challenge, *J. Geophys. Res.*, *106*, 3715–3719, doi:10.1029/1999JA900449.

Borg, A. L., M. Øieroset, T. D. Phan, F. S. Mozer, A. Pedersen, C. Mouikis, J. P. McFadden, C. Twitty, A. Balogh, and H. Rème (2005), Cluster encounter of a magnetic reconnection diffusion region in the near-Earth magnetotail on September 19, 2003, *Geophys. Res. Lett.*, *32*, L19105, doi:10.1029/2005GL023794.

Cattell, C. A., et al. (1995), ISEE 1 and Geotail observations of low-frequency waves at the magnetopause, *J. Geophys. Res.*, *100*(A7), 11,823–11,829, doi:10.1029/94JA03146.

Chaston, C. C., T. D. Phan, J. W. Bonnell, F. S. Mozer, M. Acuna, M. L. Goldstein, A. Balogh, M. Andre, and A. Fazakerley (2005), Drift-kinetic Alfven waves observed near a reconnection X line in the Earth's magnetopause, *Phys. Rev. Lett.*, *95*, 065002.

Chaston, C. C., et al. (2009), Kinetic Alfvén wave turbulence and transport through a reconnection diffusion region, *Phys. Rev. Lett.*, *102*, 015001.

Cornilleau-Wehrlin, N., et al. (2003), First results obtained by the Cluster STAFF experiment, *Ann. Geophys.*, *21*, 437–456.

Deng, X. H., and H. Matsumoto (2001), Rapid magnetic reconnection in the Earth's magnetosphere generated by whistler waves. *Nature*, *410*, 557–559.

Eastwood, J. P., T. D. Phan, S. D. Bale, and A. Tjulin (2009), Observations of turbulence generated by magnetic reconnection, *Phys. Rev. Lett.*, *102*, 035001.

Formisano, V., and C. F. Kennel (1969), Small amplitude waves in high-β plasmas, *J. Plasma Phys.*, *3*, 55–74.

Grison, B., F. Sahraoui, B. Lavraud, T. Chust, N. Cornilleau-Wehrlin, H. Rème, A. Balogh, and M. André (2005), Wave particle interactions in the high-altitude polar cusp: A Cluster case study, *Ann. Geophys.*, *23*, 3699–3713.

Gustafson, G., et al. (1997), EFW instrument for CLUSTER, in *The CLUSTER and Phoenix Missions*, edited by C. P. Escoubet, C. T. Russell, and R. Schmidt, p. 31, Springer, New York.

Howes, G. G. (2009), Limitations of Hall-MHD as a model for turbulence in weakly collisional plasmas, *Nonlin. Processes Geophys.*, *16*, 219.

Johnstone, A. D., et al. (1997), PEACE, a plasma electron and current experiment, *Space Sci. Rev.*, *79*, 351–398, doi:10.1023/A:1004938001388.

Kolmogorov, A. N. (1941), The local structure of turbulence in incompressible viscous fluid for very large Reynolds' numbers, *Dokl. Akad. Nauk SSSR*, *30*, 301–305 (reprinted in *Proc. R. Soc. A*, *434*, 9–13, 1991).

Labelle, J. A., and R. Treumann (1988), Plasma waves at the dayside magnetopause, *Space Sci. Rev.*, *47*, 175.

Narita, Y., F. Sahraoui, M. L. Goldstein, and K. H. Glassmeier (2010), Magnetic energy distribution in the four-dimensional frequency and wave vector domain in the solar wind, *J. Geophys. Res.*, *115*, A04101, doi:10.1029/2009JA014742.

Percival, D. B., and A. T. Walden (1993), *Spectral Analysis for Physical Applications*, Cambridge Univ. Press, Cambridge.

Pinçon, J. L., and F. Lefeuvre (1991), Local characterization of homogeneous turbulence in a space plasma from simultaneous measurements of field components at several points in space, *J. Geophys. Res.*, *96*(A2), 1789–1802, doi:10.1029/90JA02183.

Pinçon, J. L., and U. Motschmann (1998), Multi-spacecraft filtering: General framework, in *Analysis Methods for Multi-Spacecraft Data*, edited by G. Paschmann and P. W. Daly, pp. 65–78, Int. Space Sci. Inst., Bern, Switzerland.

Pritchett, P. L. (2001), Geospace environment modeling magnetic reconnection challenge: Simulations with a full particle electromagnetic code, *J. Geophys. Res.*, *106*(A3), 3783–3798, doi:10.1029/1999JA001006.

Rème, H., et al. (2001), First multispacecraft ion measurements in and near the Earth's magnetosphere with the identical Cluster ion spectrometry (CIS) experiment. *Ann. Geophys.*, *19*, 1303.

Robert, P., A. Roux, C. C. Harvey, M. W. Dunlop, P. W. Daly, and K. H. Glassmeier (1998), Tetrahedron geometric factors, in *Analysis Methods for Multi-Spacecraft Data*, *ISSI Sci. Rep. SR-001*, edited by G. Paschmann and P. W. Daly, pp. 323–348, Int. Space Sci. Inst., Bern, Switzerland.

Rogers, B. N., R. E. Denton, J. F. Drake, and M. A. Shay (2001), The role of dispersive waves in collisionless magnetic reconnection, *Phys. Rev. Lett.*, *87*(19), 195004.

Rönnmark, K. (1982), WHAMP–Waves in homogeneous anisotropic multicomponent plasmas, *Rep. 179*, Kiruna Geophys. Inst., Kiruna, Sweden.

Sahraoui, F., et al. (2003), ULF wave identification in the magnetosheath: k-filtering technique applied to Cluster II data, *J. Geophys. Res.*, *108*(A9), 1335, doi:10.1029/2002JA009587.

Sahraoui, F., S. Galtier, and G. Belmont (2007), On waves in incompressible Hall magnetohydrodynamics, *J. Plasmas Phys.*, *73*, 723.

Sahraoui, F., M. L. Goldstein, P. Robert, and Y. V. Khotyaintsev (2009), Evidence of a cascade and dissipation of solar-wind turbulence at the electron gyroscale, *Phys. Rev. Lett.*, *102*, 231102.

Sahraoui, F., G. Belmont, M. L. Goldstein, and L. Rezeau (2010), Limitations of multispacecraft data techniques in measuring wave number spectra of space plasma turbulence, *J. Geophys. Res.*, *115*, A04206, doi:10.1029/2009JA014724.

Sonnerup, U. O. (1979), Magnetic field reconnection, in *Solar System Plasma Physics*, vol. III, edited by L. T. Lanzerotti, C. F. Kennel, and E. N. Parker, pp. 46–108, North-Holland, Amsterdam.

Tjulin, A., J. L. Pinçon, and F. Sahraoui (2005), The k-filtering technique applied to wave electric and magnetic field measurements from the Cluster satellites, *J. Geophys. Res.*, *110*, A11224, doi:10.1029/2005JA011125.

Vaivads, A., et al. (2004), Structure of the magnetic reconnection diffusion region from four-spacecraft observations, *Phys Rev Lett.*, *10*, 1103.

Vaivads, A., Y. Khotyaintsev, M. André, and R. Treumann (2006), Plasma waves near reconnection sites, *Lect. Notes Phys.*, *687*, 251–269.

Walker, S. N., F. Sahraoui, M. A. Balikhin, G. Belmont, J. L. Pinçon, L. Rezeau, H. Alleyne, N. Cornilleau-Wehrlin, and M. André (2004), A comparison of wave mode identification techniques, *Ann. Geophys.*, *22*, 3021–3032.

Wang, X. G., A. Bhattacharjee, and Z. W. Ma (2000), Collisionless reconnection: effects of Hall current and electron pressure gradient, *J. Geophys. Res.*, *105*(A12), 27,633–27,648, doi:10.1029/1999JA000357.

Wang, X., H. A. Yang, and S. P. Jin (2006), Scalings of steady state Hall magnetohydrodynamic reconnection in high-beta plasmas, *Phys. Plasmas*, *13*, 060702.

Xiao, C. J., et al. (2007), A Cluster measurement of fast magnetic reconnection in the magnetotail, *Geophys. Res. Lett.*, *34*, L01101, doi:10.1029/2006GL028006.

Zhou, M., et al. (2009), Observation of waves near lower hybrid frequency in the reconnection region with thin current sheet, *J. Geophys. Res.*, *114*, A02216, doi:10.1029/2008JA013427.

X. H. Deng, S. Y. Huang, Y. Pang, J. F. Wang, Q. Wei, Z. G. Yuan, M. Zhou, and X. M. Zhou, School of Electronics Information, Wuhan University, Wuhan 430072, China. (monmentum82@hotmail.com)

F. Sahraoui, Laboratiore de Physique des Plasmas, CNRS-Ecole Polytechnique, Observatiore de Saint-Maur, 4 Ave. de Neptune, Saint-Maur, France.